

Physics 2700H: Lab II

Jeremy Favro (0805980), Manan Ravat (0791811), Layla Scrimgeour-Brown (0766619)

Department of Physics & Astronomy

Trent University, Peterborough, ON, Canada

February 14, 2025

Abstract

Wavelengths of emitted photons associated with electron transitions in a hydrogen atom following the Balmer series were determined utilizing both geometric and wave optics. Some results agreed within uncertainty with accepted values for these wavelengths. Minimal relative difference was noted between calculated and accepted values. Further investigation into the precision of the wave and geometric optical methods is warranted.

1 Introduction

In 1913 Niels Bohr created the Bohr model of the hydrogen atom. This model predicts that electron orbiting an atom exist only in discrete energy levels. The Bohr model of the atom provided a theoretical justification for the experimentally determined Rydberg equation which modeled the wavelength of emitted photons due to electron energy level transitions in a hydrogen atom.

In this experiment we seek to determine the wavelengths associated with electron energy level transitions between $n \geq 3$ and $n = 2$. These transitions are formally known as the H-Balmer series for a hydrogen atom and are significant as the transitions from $n \leq 5$ to $n = 2$ are easily visible to the human eye [1].

Using a hydrogen lamp a spectrally pure emission of photons of distinct wavelengths was created. Both geometrical and wave optics were employed to observe the emission spectrum of the hydrogen lamp and calculate the associated wavelengths.

2 Theory

2.1 Rydberg Equation

First stated in 1888 by Johannes Rydberg, the Rydberg equation for hydrogen relates the vacuum wavelength, λ_0 , of emitted photons due to electron energy level transitions and the initial, n_i , and final, n_f , energy levels through which the electron passes.

$$\lambda_0 = \frac{1}{R} \left(\frac{1}{n_f^2} - \frac{1}{n_i^2} \right)^{-1} \quad (1)$$

where R is the Rydberg constant [2]

2.2 Quantized Angles of Minimum Deviation

2.2.1 Geometrical Optics

Employing an equilateral glass prism enables the observation of individual wavelengths of light as each wavelength is dispersed at a different angle. See figure 3. For the study of the H-Balmer spectrum specifically a prism is utilized to determine D_m , the smallest angle achieved by varying the angle of incident light, known as the angle of minimum dispersion, which can be related to the refractive index of a prism through

$$n = \sin \left(\frac{A + D_m}{2} \right) / \sin \left(\frac{A}{2} \right) \quad (2)$$

Which, for a prism with known Cauchy constants, α and β , can be combined with Cauchy's dispersion relation

$$n = \alpha + \frac{\beta}{\lambda_{disp}^2} \quad (3)$$

to determine the wavelength of light for a given D_m

$$\lambda_{disp} = \sqrt{\left[\sin \left(\frac{A + D_m}{2} \right) / \sin \left(\frac{A}{2} \right) - \alpha \right]^{-1} \beta} \quad (4)$$

Where A is the apex angle of the prism.

2.2.2 Ray Optics

Utilizing a diffraction grating enables the study of individual wavelengths of light due to interference in the transmitted (or reflected) light created by the difference in optical path between refractions. See figure 2. For a given wavelength λ_{diff} the locations of constructive interference can be determined using

$$m\lambda_{diff} = d \sin \theta \quad (5)$$

Where m is the order of the diffracted band line, d is the spacing between lines on the diffraction grating, and θ the angle of the diffracted beam relative to the incident light.

3 Methods

3.1 Geometrical Optics

Light from a hydrogen lamp is incident on an equilateral dense flint glass prism with Cauchy constants (See equation (3)) $\alpha = 1.5935 \pm 0.8\%$ [1], $\beta = 0.0093 \mu\text{m}^2 \pm 5\%$ [1] and apex angle $A = \frac{180}{3}^\circ$. The viewing telescope, shown in figure 1, is positioned to the first ($\lambda_{theo} = 656.28 \text{ nm}$) spectral line. The table on which the prism sits, or the prism itself, is then rotated until the first spectral line reaches a reversal point at which its movement changes direction. At this reversal point, the crosshairs are aligned with the right side of the spectral line. This position is recorded using the Vernier scale. This process is repeated for the other two spectral lines, ensuring that the prism is rotated to the angle of minimum deviation for each. See figure 3 for an illustration of a successfully constructed apparatus.

3.2 Wave Optics

Light from a hydrogen lamp is incident on a diffraction grating with $k = 1.5 \times 10^4 \text{ lines/inch}$. Ideally the angle of incidence is 90° , however a method, which was not used in this experiment, to minimize error as a result of non-ideal alignment is discussed in section 4.5. The viewing telescope is positioned to the first ($\lambda_{theo} = 434.05 \text{ nm}$) spectral line and the crosshairs are aligned with the right side of that spectral line. This position is recorded using the Vernier scale. This process is repeated for the other two spectral lines. See figure 2 for an illustration of a successfully constructed apparatus.

4 Discussion

Utilizing the above methods both the prism and diffraction grating produced clear and distinct spectral lines.

4.1 Geometrical Optics

Table 1: Collected angles of minimum dispersion for an H-Lamp spectrum through a dense flint glass prism and their associated calculated wavelengths. Measurement apparatus re-zeroed between batches. δD_m taken to be $5'$ per label on apparatus.

Colour	λ_{theo} (nm)	D_m ($^\circ$)	λ_{disp} (nm)	% Diff
Red	656.28	$47.75 \pm 5'$	650.70 ± 5	0.85
Teal	486.14	$49.95 \pm 5'$	458.17 ± 5	5.9
Violet	434.05	$50.55 \pm 5'$	430.03 ± 5	0.93
Red	656.28	$48.02 \pm 5'$	614 ± 5	6.7
Teal	486.14	$49.58 \pm 5'$	478 ± 5	1.6
Violet	434.05	$50.65 \pm 5'$	426 ± 5	1.9
Red	656.28	$47.93 \pm 5'$	624 ± 5	5.0
Teal	486.14	$49.57 \pm 5'$	479 ± 5	1.4
Violet	434.05	$50.50 \pm 5'$	432 ± 5	0.43
Red	656.28	$47.75 \pm 5'$	651 ± 5	0.85
Teal	486.14	$49.50 \pm 5'$	484 ± 5	0.54
Violet	434.05	$50.47 \pm 5'$	434 ± 5	0.1
Red	656.28	$47.75 \pm 5'$	651 ± 5	0.85
Teal	486.14	$49.47 \pm 5'$	486 ± 5	0.12
Violet	434.05	$50.45 \pm 5'$	434 ± 5	0.07

Most calculated values of λ_{disp} agree within uncertainty with λ_{theo} . Overall relative difference between theoretical and observed values is low, $\approx 1.8\%$ on average, with some higher outliers exceeding the average by a significant amount.

4.2 Wave Optics

Table 2: Collected angles of diffraction for an H-Lamp spectrum through a $k = 1.5 \times 10^4$ lines/inch prism and their associated calculated wavelengths. Measurement apparatus re-zeroed between batches.

Colour	λ_{theo} (nm)	θ ($^\circ$)	λ_{diff} (nm)	% Diff
Violet	434.05	$14.50 \pm 5'$	423 ± 2.38	2.6
Teal	486.14	$16.90 \pm 5'$	492 ± 2.35	1.3
Red	656.28	$23.72 \pm 5'$	681 ± 2.25	3.7
Violet	434.05	$14.90 \pm 5'$	435 ± 2.38	0.31
Teal	486.14	$16.58 \pm 5'$	483 ± 2.36	0.59
Red	656.28	$22.60 \pm 5'$	651 ± 2.27	0.85
Violet	434.05	$14.83 \pm 5'$	434 ± 2.38	0.13
Teal	486.14	$16.63 \pm 5'$	485 ± 2.36	0.29
Red	656.28	$22.63 \pm 5'$	652 ± 2.27	0.71

Most calculated values of λ_{diff} agree within uncertainty with λ_{theo} . Initial measurements exhibit high relative error compared to later measurements, however as mentioned they are still in agreement with theoretical values.

4.3 Sources of error

In both cases a not-insignificant source of random error between repetitions of the experiment was the non-rigidity of the apparatus-lamp system. When utilizing an unfamiliar instrument in a darkened room, as was the case for this experiment, it is likely that the instrument will be concussively disturbed resulting in inconsistency between measurements taken before and after disruption. This can be avoided several ways, easiest of which is likely by constructing a mounting system for the H-Lamp which fixes it rigidly to the apparatus.

4.4 Geometrical Optics

The likely most significant source of systematic error for a prism-based system is related to the width of the slit through which the “raw” light emitted from the H-Lamp is collimated. As noted in the lab manual [1], a greater slit width results in larger and thereby more visible spectral lines however also introduces some error offset to the measured D_m . Decreasing the slit width too much causes difficulty when attempting to view and record the locations of the spectral lines.

4.5 Wave Optics

A likely significant source of systematic error here is the non-orthogonality of the light incident to the diffraction grating. By measuring the angle of diffraction of both

$+m$ and $-m$ and taking the difference of the obtained values enables the removal of this constant offset.

5 Conclusion

This experiment semi-successfully determined the easily visible, $n = 3, 4, 5$, wavelengths of the H-Balmer series to within uncertainty using both wave and geometric optics to study the spectrum of an H-Lamp.

Utilizing geometric optics λ_{disp} was determined to be (638 ± 5) nm for red, (477 ± 5) nm for blue, and (431 ± 5) nm for violet. Uncertainties taken to be the largest relative error in all variables. Only violet agrees within uncertainty with the expected value $\lambda_{theo} = 434.05$ nm. It may be worth rejecting the outliers noted in 1 with high % difference as overall most values do agree within uncertainty but those with higher % difference throw off the final result significantly.

Utilizing wave optics λ_{diff} was determined to be (661 ± 2.27) nm for red, (487 ± 2.36) nm for blue, and (431 ± 2.38) nm. Uncertainties calculated using method in section 7.1. Here both blue and violet agree within uncertainty with accepted values however, red, with the highest overall % difference does not. This is an interesting result as little effort was made during this experiment to minimize error with the diffraction grating, as seen by the non-orthogonality of the prism in figure 2. This may hint at significantly higher possible accuracies in the diffraction grating method than the prism method and is worth further investigation with greater care than was taken in this experiment.

6 Bibliography

References

- [1] Ed Stokan and Seanne Chung. PHYS-2610H lab (2025WI) the hydrogen spectrum. 2025.
- [2] Eite Tiesinga, Peter J. Mohr, David B. Newell, and Barry N. Taylor. The 2022 codata recommended values of the fundamental physical constants, 2024.

7 Appendix

7.1 Error Propagation for λ_{diff}

$$\begin{aligned}
&= \sqrt{\left(\frac{\partial \lambda_{diff}}{\partial d} \cdot \delta d\right)^2 + \left(\frac{\partial \lambda_{diff}}{\partial \theta} \cdot \delta \theta\right)^2} \\
&= \sqrt{\left(\frac{\partial \lambda_{diff}}{\partial d} \cdot \delta d\right)^2 + \left(\frac{d \cos \theta}{m} \cdot 5'\right)^2} \\
&= 5' d \cos \theta
\end{aligned}$$

7.2 Figures

Figure 1: (1) Hydrogen Lamp (2) Collimator slit, width adjustment knob at right (3) Collimating telescope, fixed (4) Diffraction grating, $k = 1.5 \times 10^4$ lines/inch (5) Viewing telescope, focusing knob at right, granular adjustment knob at bottom.



Figure 2: Illustrated first order ($m = \pm 1$) diffractions through a $k = 1.5 \times 10^4$ lines/inch, not to scale.

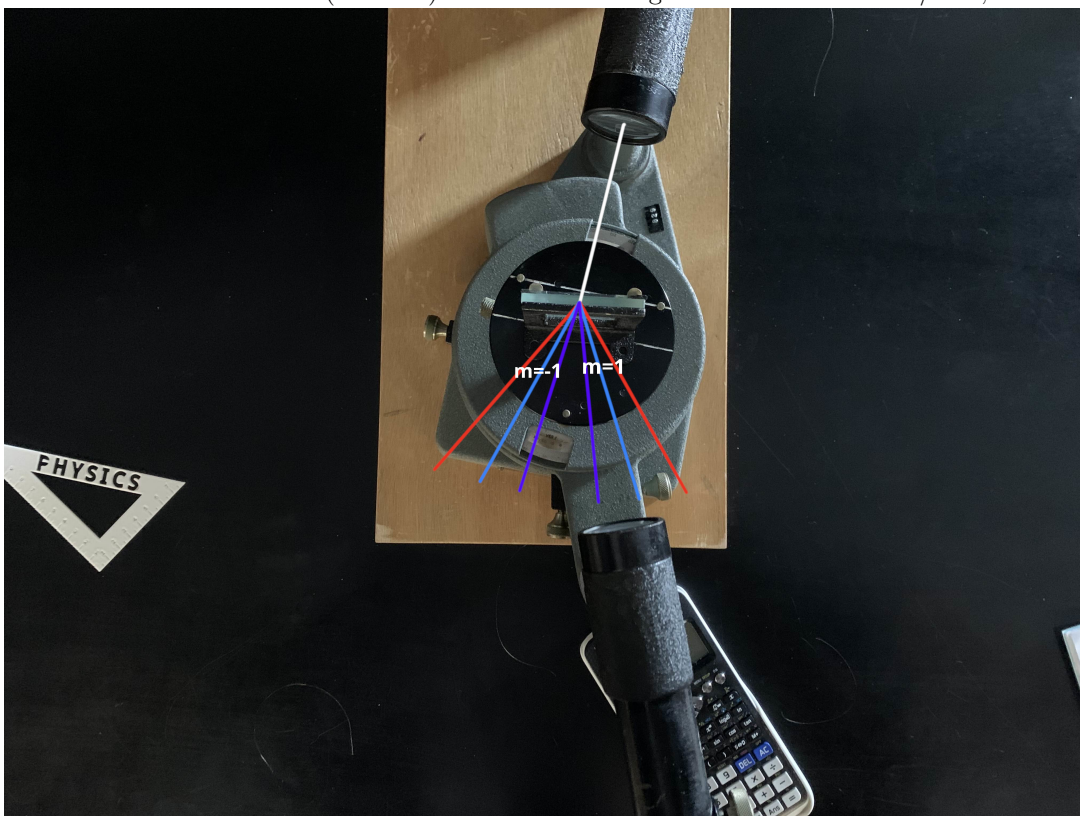


Figure 3: Illustrated angles of minimum dispersion for a dense flint glass prism, not to scale.

